Ultrasound in Med. & Biol., Vol. 31, No. 6, pp. 771–780, 2005

0301-5629/05/$–see front matter

ELSEVIER

doi:10.1016/j.ultrasmedbio.2005.01.019

● *Original Contribution*

A NEW ULTRASOUND METHOD FOR DETERMINING THE ACOUSTIC PHASE SHIFTS CAUSED BY THE SKULL BONE

JUSSI AARNIO* GREG T. CLEMENT,† and KULLERVO HYNYNEN†

*Department of Applied Physics, University of Kuopio, Kuopio, Finland; and †Department of Radiology, Brigham and Women's Hospital, Harvard Medical School, Boston, MA, USA

(*Received* 12 *September* 2004, *revised* 11 *January* 2005, *in final form* 21 *January* 2005)

Abstract—A potential noninvasive means for obtaining the value of ultrasound (US) phase shifts caused by the skull is examined. Knowledge of these shifts could be used in new methods that restore the focus from an US array after transcranial propagation. In the present study, a pulsed signal was emitted from a single element of a therapeutic US transducer. The reflected signal was then recorded. The data were examined over the band width of the transducer, producing amplitude data as a function of frequency. A periodic appearance of local maxima and minima was observed in the data as a function of frequency. We hypothesize that the amplitude is primarily determined by the superposition of the reflections between the interfaces at the inner and outer surfaces of the skull and between the interior interfaces of trabecular and cortical bone. A homogeneous-layer model was used to predict the forward-propagated phase using the reflection data. Good correlation was found between the numeric calculation and phases measured after propagation through single-layer plastic plates. The method was used on curved three-layer plastic phantoms and four excised human skulls. The procedure could eventually be applied toward phasing multielement arrays. Such an application could have implications in both therapeutic and diagnostic brain procedures. (E-mail: gclement@hms.harvard.edu)

Key Words: **Ultrasound, Transskull therapy, Noninvasive, Phase shift, Reflection.**

INTRODUCTION

Ultrasound (US) has been used extensively in medicine since the introduction of diagnostic US (Erikson et al. 1974; Kremkau 1979). Despite its use in physical therapy and medical diagnostics, US is capable of many therapeutic operations that remain relatively unknown. Its capability to focus high intensities of energy into a small target deep in tissue (ter Haar 1995) has allowed its use in a wide range of hyperthermic and noninvasive surgical procedures.

The prospect of noninvasive brain treatments is particularly exciting. In the 1950s, Fry et al. (1954) and Barnard et al. (1955, 1956) produced lesions in the central nervous system with focused US. However, in these early ultrasonic operations in the brain, a soft tissue window was required because skull bone was considered to be impenetrable. This was achieved by removing a piece of skull before operation. Later, in the 1970s, Fry (1977) was able show that enough ultrasonic energy can be focused through a piece of human skull to produce thermal lesions into a lucite block. He used a single-element transducer at the frequency of 1 MHz. Although his experiments were otherwise successful, the focus was shifted by 2 to 3 mm after a piece of skull was inserted between the transducer and the lucite block. Fry and Goss (1980) produced lesions into lucite and into a cat brain through a piece of human skull by using an US single-element transducer at 500 kHz. However, they did not consider either the exact placement of the lesion or the temperature rise at the skull. This indicates that the problems associated with the misplacement of the focus and temperature rise at the skull were not solved by that time.

More recently, the combined development of magnetic resonance imaging (MRI)-guided US and high-power phased arrays has offered a new tool for brain treatments (Ebbini et al. 1988; Vykhodtseva et al. 2000). Vykhodtseva et al. (2000) showed that MRI thermometry can reliably predict irreversible brain tissue damage. Meanwhile, phased arrays have addressed the problems

Address correspondence to: Dr. G. T. Clement, Dept. of Radiology, Brigham and Women's Hospital, Harvard Medical School, 221 Longwood Ave., Rm. 521, Boston, MA 02115 USA. E-mail: gclement@hms.harvard.edu

associated with defocusing caused by the skull (Hynynen and Jolesz 1998; Sun and Hynynen 1998, 1999; Clement et al. 2000a, 2000b). Hynynen and Jolesz (1998) destroyed rabbit brain tissue *in vivo* through a piece of human skull with a single-element transducer, without excessive heating of the skull bone. With a multielement transducer array, they were able to show that the focus through a skull can be reconstructed to the intended focus, even at frequencies at which it is completely destroyed when a conventional single-element transducer is used. Clement et al. (2000a) further investigated the use of US in brain therapy, and found that a large hemispherical array was able to produce thermal lesions in a rabbit thigh muscle through human skull, without overheating the skull.

To make phased arrays effective in focusing US through inhomogeneities, each source element in the array requires its own phasing information. The aim of phasing is to make the sound beam originating from each element arrive at the intended focus in phase, to produce constructive interference. In the case of focusing through a human skull, mildly invasive (Thomas and Fink 1996; Tanter et al. 1998; Seip et al. 1994; Clement and Hynynen 2002a) and completely noninvasive (Sun and Hynynen 1998, 1999; Hynynen and Sun 1999; Clement and Hynynen 2002b, 2002c; Aubry et al. 2001, 2003; Pernot et al. 2001) means have been presented. In studies by Thomas and Fink (1996) and Tanter et al. (1998), focus was restored by time-reversal mirror (T-RM), in which an acoustic source was put into the desired focal spot, and the sound waves originating from it were recorded with the intended treatment array time-reversed and emitted. The emitted sound waves will focus optimally into the original target, but the method requires implanting a sound source into the treatment volume. Catheter-inserted hydrophones were used by Seip et al. (1994) and by Clement and Hynynen (2002a) to acquire the required phase correction. In this method, the phase correction is measured at one point inside the brain and the required correction for the treatment volume is calculated. The advantage of this method is that it does not require precision placement of the hydrophone, which can be placed inside the brain through the vascular system. An MRI-based method for noninvasive focusing was proposed by Sun and Hynynen (1998, 1999) and Hynynen and Sun (1999). In their numeric study, a skull model was digitized from MR images and it was considered to be a single layer. Methods for deriving the required correction from computerized tomography (CT) scans were proposed by Clement and Hynynen (2002b, 2002c); Aubry et al. (2001, 2003) and Pernot et al. (2001). Clement and Hynynen (2002b) developed a model that uses information from the CT images to predict the propagation of US in the skull. The model was used with a homogeneous skull with both normal and oblique angles of incidence. Predicted phase corrections were then used in focusing US through 10 *ex vivo* skulls. Image-derived phase correction was also compared with correction obtained with hydrophone feedback. Their results show that algorithms used in phase correction are able to reconstruct the destroyed focus and reduce the side-lobe level by 50% from the uncorrected case. Better focus, evaluated in shape, location and peak pressure amplitude, was gained by using these algorithms. CT-image-derived phase correction was also used by Clement and Hynynen (2002c), in which the density-dependent speed-of-sound (SOS) was taken into account and both one- and three-layered skull models were studied. With density-dependent SOS, models predicted peak acoustic pressures of 76% and 79% of the ideal peak pressure amplitudes for one- and three-layer models, respectively. Aubry et al. (2003) and Pernot et al. (2001) used 3-D finite differences numerical simulation of the complete wave equation to exploit all the information in the CT scans. Rather than modeling skull with one or three layers, they analyzed CT images at each pixel. Their approach was similar to T-RM but, instead of using a physical sound source at the intended focus, they used a virtual source. The numerically-derived wave-front was found to be very close to the one that was experimentally acquired. The time-reversal process of focusing through heterogeneities is improved with the spatiotemporal inverse filter presented by Aubry et al. (2001).

Despite the advances in T-RM-, MRI- and CT-based focal restoration, these methods proposed so far have either been rather complex or not completely noninvasive. In addition, the skull properties vary from patient to patient and location to location in each patient. Although the use of the bone density decreases this variation, the phase corrections are not perfect (Clement and Hynynen 2002c), and methods allowing direct measurement of the SOS in each skull location would improve the focusing.

The purpose of our work was to develop a simple and fast US method capable of determining the acoustic phase shifts in skull bone noninvasively. By recording the reflected signal and calculating its frequency spectrum, the phase distortion of the object in the sound beam can be determined and compensated. The method is based on the thickness resonance of an object (Guyott and Cawley 1988) when pulse excitation is used. A similar approach was used by Ohkawai et al. (1983) in measuring the thickness or the SOS in the heart valves of a dog *in vivo*.

Using the resonance US method on plastic plates and human skulls *ex vivo*, we showed that the resonance method provides a noninvasive means for determining

the acoustic phase shifts. The method proposed in this paper is simple and fast to perform. Patient safety is promoted because the measurement is performed at the acoustic pressure level equal to that of diagnostic US. We hypothesize that the resonance method could have an application in noninvasive transcranial focal restoration.

THEORY

The theory of sound beam propagation in the layered medium is covered in detail by Brekhovskikh (1960) and by Kinsler et al. (2000), of which the latter is followed in this paper. When a sound wave arrives at the boundary of two media, it experiences reflection and refraction, phenomena that are well-known from the optics. In the sound-wave case, the acoustic impedances of these two media determine how much of the incident wave is reflected back and what fraction of it is transmitted into the other medium. The acoustic impedance of bone is significantly larger than that of soft tissue, which makes it a strong acoustic reflector.

Even though bone is a good reflector for a sound wave coming from water or acoustically water-like medium, not all of the initial wave is reflected; a part of it is transmitted into bone. This transmitted wave will interact at the second boundary, the bone-soft tissue boundary at the far side of the bone. Again, part of the wave is transmitted and part is reflected, and the reflected part eventually reaches the transducer.

A pressure wave propagating in a medium can be written as:

$$p = Pe^{j(\omega t - kx)} \tag{1}$$

where P is the amplitude of the oscillation, ω is the angular frequency, k is the wave number and x is the distance from the origin.

Accordingly, pressure waves can be written for transmission and reflection, and algebraic manipulation of these waves leads to the pressure-reflection coefficient:

$$R = \frac{j\left(\frac{z_b}{z_w} - \frac{z_w}{z_b}\right)\sin k_b d}{2\cos k_b d + j\left(\frac{z_b}{z_w} + \frac{z_w}{z_b}\right)\sin k_b d}, \tag{2}$$

where z_w is the acoustic impedance of the water, z_b is the acoustic impedance of the bone, k_b is the wave number in bone and d is the thickness of the bone sample. This is the pressure-reflection coefficient at the first boundary. And, for the intensity-transmission coefficient,

$$T_I = \frac{1}{1 + \frac{1}{4}\left(\frac{z_b}{z_w} - \frac{z_w}{z_b}\right)^2 \sin^2 k_b d}. \tag{3}$$

For the special case that $k_b d = n\pi$, total transmission occurs; that is, $T_I = 1$ for frequencies:

$$f_i = n\frac{c_b}{2d}, \tag{4}$$

and where n is integer 1, 2, . . . and cb is the SOS in the bone.

In a lossy medium, this is not actually a total transmission but, rather, an increased transmission. Frequencies f_i are the resonant frequencies of the bone layer.

If a bone sample in the water bath is investigated with an ultrasonic pulse, the transducer sends a distribution of frequencies, the magnitude of which depends on the pulse shape, length and transducer properties. As we saw above, at resonant frequencies of the sample there is increased transmission; that is, the sound wave travels through the sample and enters into medium behind the bone. Therefore, a transducer at one side of the bone that investigates the sample with an ultrasonic pulse receives an echo that does not have the resonant frequencies of the sample in it and, thus, the frequency spectrum of the received signal will show minima at those frequencies.

The equation for the SOS in bone can be derived from eqn (4). Measuring two adjacent resonance-frequency minima from the frequency spectrum of the received echo, and knowing the thickness of the bone sample, the SOS in the bone can be calculated by:

$$c_b = 2d\,(f_{i+1} - f_i) = 2d\Delta f\,. \tag{5}$$

The term $(\omega t - kx)$ in eqn (1) is called the phase. Further manipulation of phase leads to a form:

$$(\omega t - kx) = \left(\omega t - \frac{2\pi f x}{c}\right), \tag{6}$$

where f is the frequency and c is the SOS in the medium.

Therefore, we can write the following equations for phases in water and in bone at distance $x = d$:

$$\phi_w = \omega t - \frac{2\pi f d}{c_w} \tag{7a}$$

$$\phi_b = \omega t - \frac{2\pi f d}{c_b}\,. \tag{7b}$$

Phase difference between these two waves is:

$$\Delta\phi = \phi_w - \phi_b = 2\pi f\left(\frac{1}{2\Delta f} - \frac{d}{c_w}\right), \tag{8}$$

where c_b is substituted with eqn (5).

This can be thought of as a phase shift caused by a bone layer of thickness d. In a practical case, the frequency is known and SOS in water is well studied; several sources can be found to calculate the phase shift (Kinsler et al. 2000;

Del Grosso and Mader 1972). The thickness of the skull can be measured noninvasively by using modern imaging techniques and the SOS in the bone can be calculated with eqn (5). Equation (8) forms the basis for measuring the phase shift with the transducer.

MATERIALS AND METHODS

Materials

The materials studied consisted of 12 pieces of acrylic plastic sheets, three pieces of polycarbonate plastic sheets and four human skulls *ex vivo*. In addition to these materials, four sheets of acrylic, four sheets of polycarbonate and five sheets of soft polyvinyl chloride (PVC) were used in three-layer plastic phantoms.

The thickness of each plastic sheet was measured 10 times and a mean thickness was calculated. Calculated thickness values of sheets used in the single-layer experiments varied, in the case of acrylic pieces, from 2.8 to 11.8 mm and, in the case of polycarbonate pieces, from 2.8 to 9.1 mm. Thicknesses of acrylic pieces used in the three-layer phantoms varied from 2.0 to 3.9 mm, whereas the polycarbonate pieces thicknesses ranged from 1.9 to 5.7 mm and PVC sheets from 1.8 to 4.8 mm. Thicknesses of the samples were measured by using a digital caliper (Mitutoyo Absolute Digimatic digital caliper model CD-6" CS, Kawasaki, Japan).

The purpose of the three-layer plastic phantoms was to mimic the structure of the skull bone. In skull bone, the first and third layers are of dense cortical bone, in which the SOS is higher than in the middle layer, also called diploë (Fry and Barger 1978). The SOS in acrylic (Wells 1977) is higher than that in polycarbonate plastics (Hung and Goldstein 1983) or PVC, the SOS in which was measured to be 1770 m/s $\pm$ 130 m/s and, therefore, the first and third phantom layers were selected to be of acrylic and the layer in the middle was of either polycarbonate or PVC. Sheets were clamped together underwater to inhibit the presence of air bubbles in between the sheets.

After flat three-layer phantoms were measured, each acrylic and polycarbonate plate used in the phantoms was bent, using an oven and a mold made in-house. The mold had a radius of curvature of 8 cm. Acrylic plates were heated at 115 °C for 15 min each and polycarbonate plates at 160 °C for 10 min. Plates were allowed to cool down while they were kept compressed in the mold. Curved three-layer phantoms were composed and measured in a similar manner used for flat phantoms. Thickness of each plate was measured after bending. Measurements showed that the thickness of the two thinnest acrylic plates and the polycarbonate plate IV had increased by 0.1 mm, but the thickness of the rest of the plates had remained unchanged. This increase in the thickness of these three plates is about half of the error of the thickness and, therefore, the thickness of each of the plates can be assumed not to have changed during the bending process. The thickest PVC sheet was not used with curved acrylic plates because it was too thick and stiff to be used with the those plates.

Skull samples were four adult skull caps *ex vivo* fixed in formalin. Based on a study by Fry and Barger (1978), the acoustical properties of a skull fixed in formaldehyde are assumed to be similar to the properties of a fresh skull. The skulls are referred to here as SK1–SK4. On the skull surfaces, there were points marked with ink from previous studies. The thickness of those points had been measured using a mechanical caliper and the results from those measurements were also used in this study. All skulls used in this study were of one piece, three of which consisted of the whole skull cap, and one consisted of the right half of the skull cap. Neither the gender nor exact ages of the cadavers were known. No visible damage or malformation was observed.

Equipment

The experiment setup consisted of a digital oscilloscope (Yokogawa DL 7100, Tokyo, Japan), ultrasonic pulser and receiver (Panametrics model 500PR, Waltham, MA, USA), arbitrary waveform generator (Wavetek model 395, Fluke Precision Measurement Ltd., San Diego, CA, USA), a nine-element nonfocused broadband ultrasonic transducer array (Imasonic, Lyon, France), in-house assembled 1-mm diameter lead zirconate-titanate (PZT)-hydrophone (Penn State Material Science Department, State College, PA, USA) and computer. The computer was connected to the oscilloscope with a general purpose interface bus (GPIB) cable, and measured signals were saved to the computer hard drive for off-line analysis. Water temperature was monitored during all experiments with a mercury thermometer.

The elements on the nine-element array were equal in area and consisted of a center piston with surrounding ring divided into eight elements. All elements of the nine-element array were driven at the same phase and with the same driving signal; thus, making it operate as a single-element transducer. The transducer diameter was 29.2 mm and radius of curvature 150 mm. The center frequency of the transducer was 900 kHz and usable in the frequency range from 0.60 MHz to 1.74 MHz. The transducer used to measure the three-layer plastic phantoms was a 19-mm diameter, single-element planar nonfocused transducer with the center frequency of 1 MHz and usable in the frequency range from 0.35 MHz to 1.6 MHz (V314, Panametrics).

Other equipment used only in the experiments with the three-layer phantoms was a 1-mm polyvinylidene difluoride (PVDF) hydrophone (Precision Acoustics, Wakefield, UK), HP 54615B digital oscilloscope

(Hewlett Packard, Palo Alto, CA, USA), Agilent 33120A function generator (Agilent Technologies, Palo Alto, CA, USA) and a DC power supply for the hydrophone preamplifier.

Experiments

Targets (plastic or skull) were placed approximately 8 cm in front of the transducer. For stability, plastic sheets were clamped into the aluminum mounting stand. Before measurements, skulls were affixed to a plastic frame, allowing them to attach to the mounting stand. A connecting bar coupled the transducer and the hydrophone and allowed the incident angle of the beam to be adjusted without losing the alignment between the transducer and hydrophone. The distance between the transducer and the tip of the hydrophone was approximately 14.5 cm.

Two kinds of measurements were made. First, a sharp ultrasonic pulse was reflected off a target surface and displayed on the oscilloscope screen. The pulse consisted of one negative peak with peak amplitude of −250 V, pulse duration of 1.3 μs and 180-kHz center frequency. The reflected waveform was then saved to the computer, after which a frequency spectrum of the signal was calculated off-line. The transducers used in the study did not allow a wider range of frequencies than those mentioned above. Pulsing was done with the ultrasonic pulser (Panametrics). The SOS in the sample was calculated from the frequency spectrum using eqn (5) and the phase shift using eqn (8). The SOS in water was calculated by using the experimental equation (Del Grosso and Mader 1972). The set-up for this experiment is shown in Fig. 1a.

Second, the phase shift was measured with the hydrophone. The signal through the target was measured, after which the target was removed from the experiment tank and the signal in only water was measured. The phase difference was determined directly from these two signals. The transducer input for the hydrophone measurements was generated in the arbitrary waveform generator (Wavetek); it was a 20-period sinusoid at 810 kHz. Figure 1b shows the set-up for this experiment. The pulser and receiver (Panametrics) had a built-in amplifier for the incoming signal, and it acted as an amplifier in this set-up. In the experiments with the three-layer phantoms, the 20-period sinusoid was generated in the Agilent function generator. For comparison, the mean SOS was calculated from the hydrophone signals and compared with the reflection-calculated one.

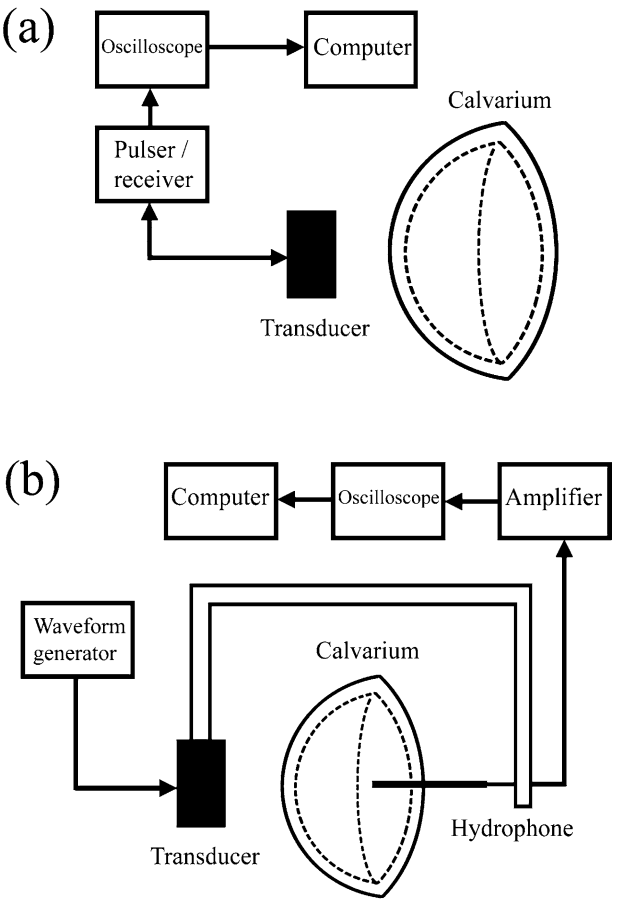

Fig. 1. Experimental set-ups for (a) reflection measurements and (b) hydrophone measurements. The hydrophone-measured phase shifts were measured in through-transmission mode.

RESULTS

Single-layer plates

Altogether, 56 signals of the single-layer plastic plates were studied. Reflected signal from the 8.09-mm thick acrylic plate and the normalized frequency spectrum of it are shown in Fig. 2. All minima locations from the spectrum were measured, and the SOS was calculated for each case. An average speed was used in the phase shift calculations in eqn (8). Further, an average of predicted SOS values in acrylic plates was calculated from both the reflection- and the hydrophone-measured data. The reflection data revealed a mean speed of 2769 m/s ± 41 m/s (SD), whereas the hydrophone data yielded a mean speed of 2754 m/s ± 108 m/s (SD). Both of the calculated mean speeds were about 3% higher than the 2680 m/s reported by Wells (1977), but were acceptable because some variation occurs in the materials because of the different manufacturing techniques.

The phase shift was calculated from both the reflected and transmitted signals. Because the target object was not moved between recording of the reflection and hydrophone measurement, these quantities should equal each other. The calculated phase shifts in the single-layer plastic sheets are plotted against each other in Fig. 3. The hydrophone-measured phase shift can be thought of as an

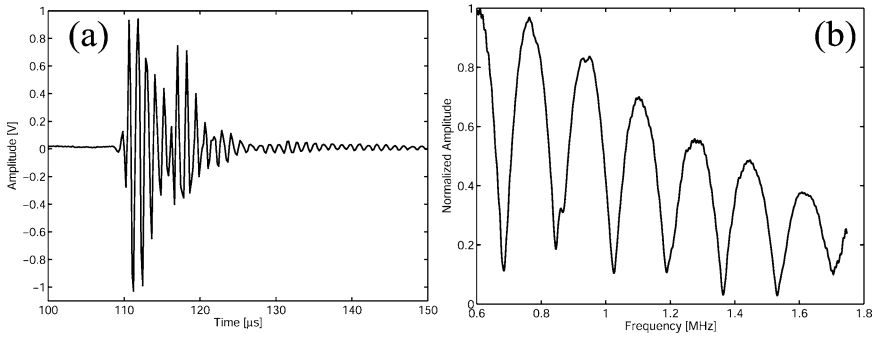

Fig. 2. (a) Measured radiofrequency (RF) signal and (b) normalized frequency spectrum of the reflected signal from 8.09-mm thick acrylic plate. In addition to longitudinal modes, some shear modes are excited as well and are seen in (b). The presence of shear modes indicates the slight deviation of the sound beam from normal angle of incidence.

actual phase shift. Therefore, the difference between the transducer-measured phase shift and the hydrophone-measured shift determines the accuracy and usability of the new measuring modality. The transducer-measured phase shift was subtracted from the hydrophone measure, an absolute value was taken of it and, after that, an average was calculated. In the case of the single-layer plastic plates, the mean difference between the two modalities was calculated to be 12.2° ± 9.6° (SD).

Three-layer phantoms

The three-layer plastic phantoms were studied in a similar set-up to that for the single-layer plates, both before and after bending them. Before the plates were bent, the reflection-calculated phase shifts differed from the hydrophone-measured phase shifts by an average of 28.5° ± 25.4° (SD). After bending of the plates, the mean difference between the two modalities was 36.6° ± 34.6° (SD). Results from the experiments are shown in Figs. 4 and 5, before and after bending the plates, respectively.

Skulls

Similar experiments were done by using four human skulls *ex vivo* as target objects. The skulls were placed on an in-house made stand that allowed rotation of the skulls and, therefore, made it possible to study the most distant points with a single-element transducer. Normalized frequency spectra of signals recorded after they were reflected off six different skull locations are shown in Fig. 6. The best, typical, bad and the worst cases of skull spectra are presented. The best-case scenario is shown in Fig. 6a, where a clear resonance pattern can be observed. Figure 6b through d represents typical

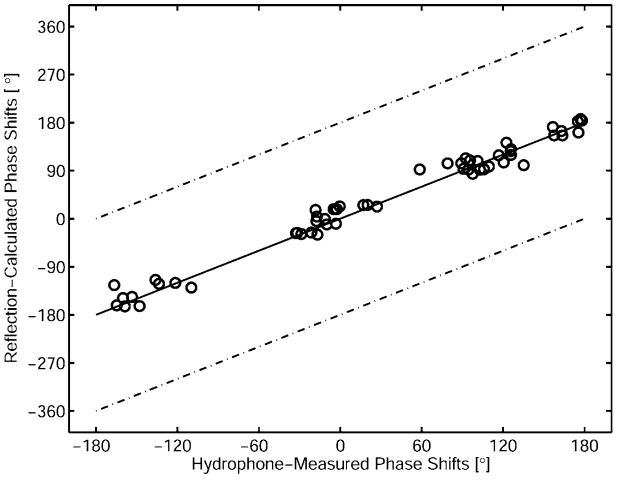

Fig. 3. Transducer-calculated phase shifts (°) as a function of hydrophone-measured phase shifts (°) in single plastic plates. Lines indicate deviation of ± 180° in phase and (middle) 1:1 correspondence between two modalities.

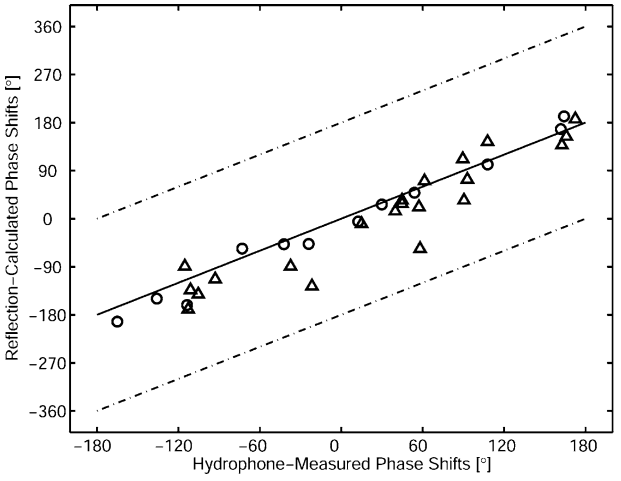

Fig. 4. Transducer-calculated phase shifts (°) as a function of hydrophone-measured phase shifts (°) in flat three-layer plastic phantoms. (○) Phantoms consisting of acrylic-polycarbonate-acrylic plates; and (△) acrylic-PVC-acrylic phantoms.

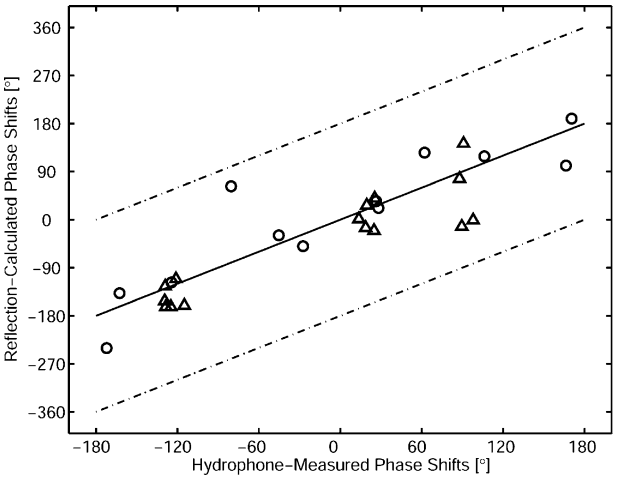

Fig. 5. Transducer-calculated phase shifts (°) as a function of hydrophone-measured phase shifts (°) in curved three-layer plastic phantoms. (○) Phantoms consisting of acrylic-polycarbonate-acrylic plates; and (△) acrylic-PVC-acrylic phantoms.

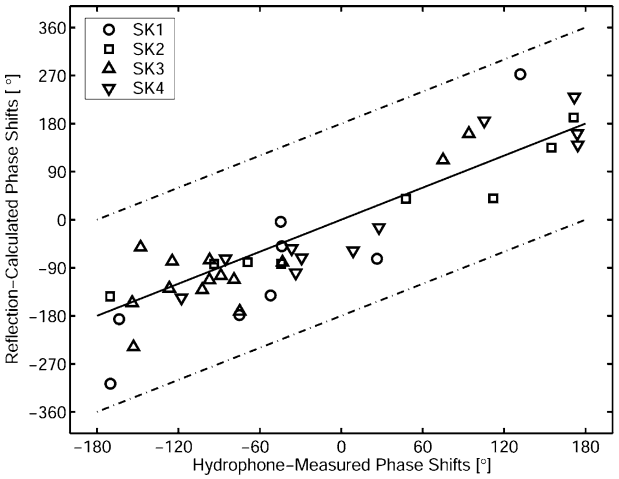

Fig. 7. Transducer-calculated phase shifts (°) as a function of hydrophone-measured phase shifts (°) in skulls SK1–SK4.

cases with different degrees of degradation. Attenuation at higher frequencies degrades the spectrum in the region above 1 MHz, but clear resonances are separable at lower frequencies. Figure 6e shows a degraded spectrum with hardly visible resonances; however, four resonance frequencies can be separated from wide minima locations. The worst-case spectrum is shown in Fig. 6f, where most of the spectrum is distorted and hardly any resonances are visible.

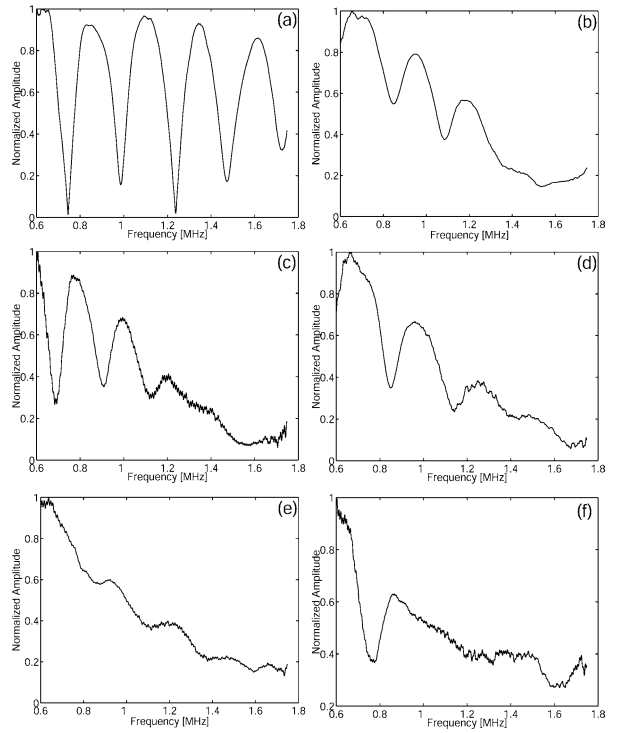

Fig. 6. Normalized frequency spectra from six different skull locations, showing different amounts of spectrum degradation. (a) Near ideal spectrum and (b)–(d) typical spectra, where resonances are clearly visible, but spectra are degraded in the region above 1 MHz. (e) The spectrum is highly degraded, but resonances can be separated, whereas in (f) the spectrum is unusable.

The mean of reflection-calculated SOS values were calculated and compared with those that were hydrophone-calculated. Reflection measurements yielded a mean SOS of 2830 m/s ± 520 m/s (SD), whereas hydrophone data yielded 2674 m/s ± 330 m/s (SD); thus, in this experiment, the resonance method predicted an average of 5.8% higher SOS values than did the through-transmission measurements done with the hydrophone.

In Fig. 7 is shown the results from the experiments with four skulls, demonstrating a good correlation between the measured and the calculated phases. The mean difference was 46° ± 40° (SD).

DISCUSSION

The results from this preliminary study indicate that the US reflection measurement may have an application in transcranial focusing. The SOS in a studied object is determined by measuring the resonance frequencies of the object and phase shifts are calculated. The method proposed is completely noninvasive and fast to perform.

In our initial experiments, the method was consistently able to predict the phase of the hydrophone-measured shifts through the single-layer plates. The maximum phase discrepancy experienced in all 56 measurements was 43° and, in 44 samples, this difference was less than 20°. The purpose of the three-layer phantom experiments was to fill the gap between the single-plate

experiments and skull experiments. As expected, the three-layer phantoms showed increased discrepancy between the two modalities in comparison with the single-layer case, but this was smaller than with skulls. Further on, it was expected to see the difference between the modalities increase after the plates were bent. In the case of flat phantoms, the results show that, in 42% of the differences, the discrepancy between modalities was less than 20° and, in 18%, it was less than 10°. In the curved phantoms, the corresponding percentages were 44% and 22%, respectively. This clearly shows that the method presented here can also predict the phase shifts in complicated structures.

In skull experiments, the mean difference between hydrophone-measured and transducer-measured phase shifts is greater, leading to a mean difference of greater than 45°. There can be seen a slight systematic bias and an increased error trend for large phase shifts in the results in Fig. 7. The systematic bias is believed to originate from the error in the thickness of the skull. The diameter of the transducer used in the skull experiments was 29.2 mm, large enough for the thickness variation in skull bone not to be considered to be negligible. The resonance method predicted on average 5.8% higher SOS values than those measured with the hydrophone in through-transmission. The discrepancy was expected to be induced by the measurement geometry. The needle-hydrophone–measured SOS values correspond to the SOS at the geometric center of the sound beam, whereas the reflection-calculated SOS values correspond to average SOS over entire area of the sound beam. Any thickness variation in the skull bone across the sound beam leads to variation in the SOS and, thus, increases the discrepancy between the reflection- and hydrophone-measured SOS. It is interesting to note that, when reflection-calculated SOS values were compared with the mean of those given for skulls by Fry and Barger (1978), the difference was 1.5%. Despite the bias, out of 41 sample points, nearly 65% differed by less than 45° and nearly 30% of the measurements were less than 20° different from the hydrophone measurement. Sound waves with phase differences of less than 20° will still act constructively and, thus, provide an improvement in the focus from the uncorrected case. The reason for the increase in the error trend for large phase shifts is not clearly known; however, it is suspected that increased bone thickness was affecting the phase-shift measurements, causing error in the results. The effect was only observed with skull samples and not with single- or three-layer plates; therefore, it is reasonable to suggest that skull structure and geometry were inducing the error.

The method proposed is closely similar to resonant US spectroscopy (RUS), widely used in material testing (Maynard 1996; Leisure and Willis 1997; Schwarz and Vuorinen 2000). According to Maynard (1996), the term "resonant ultrasound spectroscopy" comprises all the techniques that use ultrasonic resonance frequencies to determine the elastic moduli. Generally, in RUS, the studied sample is held lightly in between two transducers that are in contact with the sample, but there are also some noncontact RUS methods available (Schwarz and Vuorinen 2000). However, these methods are not applicable in transcranial focusing. Because RUS is widely used in material testing and the procedures involved with it are specific, it would be misleading to call the method presented in this paper as a RUS method because the method presented here does not use contact transducers, nor is it used for solving the elastic constants of material.

Acoustical properties of structures have been also studied by Kinra et al. (1994) and Yapura et al. (2004), who used resonance frequencies of layered structures to determine the acoustic properties of materials. Their approach is in the field of inverse problems. Kinra et al. (1994) solved simultaneously the thickness and the wave speed, whereas Yapura et al. (2004) solved the traveling times and the acoustic impedances; both studies were done using acoustically thin three-layered structures. The accuracy of such an inverse method is reported to be very impressive, $\pm$ 2% in the SOS.

Skull bone imposes a demanding challenge for any method used in determining the SOS. The direct time-of-flight measurements in skull would be possible only at some areas of skull, because of the high SOS and acoustic attenuation in bone. If practical focused US therapy through the skull is to be given with a hemispherical array (Clement et al. 2000b; Clement and Hynynen 2002b), oblique angles of incidence are expected and sound beams are reflected to directions other than those of the emitting transducer. Clearly, the method used in measuring the SOS has to work in all cases, not just in easy ones. There are also some other pulse-echo methods for determining the SOS (Anderson and Trahey 1998; Ophir 1986), but neither these nor the methods that use through-transmission (Strelitzki et al. 1996) are applicable in noninvasive determination of the SOS in skull bone with a focused US surgery array. The main disadvantage with methods proposed by Anderson and Trahey (1998) or Ophir (1986) is that, in those methods, either the array needs to be moved or the measurement geometry rules out the use of hemispherical arrays and strongly curved objects, such as the human skull, whereas the methods using the technique of through-transmission are excluded as being invasive.

Results of our experiments showed that the error of the proposed method increases when the geometry of the object becomes more complicated. This was seen with both three-layer phantoms and with skulls. The increase in the discrepancy between the two modalities in the

experiments with skulls compared with those with three-layer phantoms is believed to be related to the more complicated structure of bone and to the 2-D curvature of the skull surface. Furthermore, the experiments with three-layer phantoms were done with a smaller transducer, which affects the discrepancy as well. If the diameter of the transducer used is too big, the curved surface may no longer be considered to be flat. A curved surface reflects parts of the incoming wavefront to directions other than that of the emitting transducer, causing the signal-to-noise ratio (SNR) to decrease. Further, if the radius of curvature of skull is assumed to be 80 mm and the sound beam of a planar transducer is assumed to be the size of the transducer element, then, at the edges of the sound beam, an angle of incidence of about 11° between a 29.2-mm wide sound beam and the skull surface can be expected. This angle of incidence at the edges of the sound beam reduces to 7° if a transducer of 19 mm in diameter is used. The sizes of transducers are those used in this study. It is evident that the skull data presented in this paper are degraded by the size of the transducer used and that the assumption of flat skull surface used in the work is invalid. Clearly, it would be preferable to use a smaller-diameter transducer in experiments with skulls than was used in this work but, unfortunately, because of hardware limitation, it was not possible at the time these experiments were carried out. The choice of the transducer is a trade-off between wide band width and low center frequency. Skull bone dictates the frequencies that can be used and, as is seen in Fig. 6, the frequencies above 1 MHz are distorted. Transducers with lower center frequency would offer an increase of SNR in the data but, unfortunately, also a narrower band width.

The purpose of this study was to show that the phase shifts can be measured with pulsed US in skull bone. The advantages of the proposed resonance method in determining the acoustic phase shifts in skull bone are that it is completely noninvasive, simple, fast and safe to the patient. The resonance method produces the effective SOS in the studied sample directly with US, rather than by calculating it from CT image densities. The other methods currently available for the task rely on heavy and complicated computing, or are not entirely noninvasive. It should be noted, however, that, at its present stage, the resonance method is dependent on the CT or other modern imaging modality to provide the thickness of the skull. The effectiveness of the proposed resonance method in predicting the SOS in bone as compared with the other methods, especially the CT-based methods, and developing the method to be completely independent of other modalities are matters of future work. Future work also includes the comparison of the reflection-calculated SOS with that derived from CT images. We hypothesize that, if the method were used toward the focal restoration in transcranial focusing, an improvement in processing time would be expected. Further, the future investigation includes the evaluation of the focusing quality gained with the proposed method. Numeric compensation for skull curvature and incident angle may be possible by using reflection data from multiple elements in a transducer array.

CONCLUSIONS

A new method for determining the phase shift caused by the skull is presented. The method is completely noninvasive and requires no additional investments in treatment devices. It is also safe to the patient, because it does not require high-power US beams or long sonication times. This method may be useful in online measurement of the SOS in the skull bone and, thus, allow a method to tune the focusing algorithm for each patient and location of the skull. This could lead to a significant improvement in the transskull US treatments of the brain.

*Acknowledgements*This work was supported by the National Institutes of Health (grant CA 76550), the Academy of Finland (grant 44042), the Finnish Cultural Foundation North Savo Fund, and Kouvolan Sivistys-ja Urheilutalo Säätiö.

REFERENCES

Anderson ME, Trahey GE. The direct estimation of sound speed using pulse-echo ultrasound. J Acoust Soc Am 1998;104:3099–3106.

Aubry J-F, Tanter M, Gerber J, Thomas J-L, Fink M. Optimal focusing by spatio-temporal inverse filter. II. Experiments Application to focusing through absorbing and reverberating media. J Acoust Soc Am 2001;110:48–58.

Aubry J-F, Tanter M, Pernot M, Thomas J-L, Fink M. Experimental demonstration of noninvasive transskull adaptive focusing based on prior computed tomography scans. J Acoust Soc Am 2003;113:84–93.

Barnard WJ, Fry WJ, Fry FJ, Brennan FF. Small localized ultrasonic lesions in the white and gray matter of a cat brain. Arch Neuro Psychiatr 1956;75:15–35.

Barnard WJ, Fry WJ, Fry FJ, Krumins RF. Effects of high intensity ultrasound on the central nervous system of the cat. J Comp Neurol 1955;103:459–484.

Brekhovskikh LM. Waves in layered media. New York: Academic Press, 1960.

Clement GT, Hynynen K. Micro-receiver guided transcranial beam steering. IEEE Trans Ultrason Ferroelec Freq Control 2002a;49:447–452.

Clement GT, Hynynen K. A non-invasive method for focusing ultrasound through the human skull. Phys Med Biol 2002b;47:1219–1236.

Clement GT, Hynynen K. Correlation of ultrasound phase with physical skull properties. Ultrasound Med Biol 2002c;28:617–624.

Clement GT, Sun J, Giesecke T, Hynynen K. A hemisphere array for noninvasive ultrasound brain therapy and surgery. Phys Med Biol 2000a;45:3707–3719.

Clement GT, White J, Hynynen K. Investigation of a large-area phased array for focused ultrasound surgery through the skull. Phys Med Biol 2000b;45:1071–1083.

Del Grosso VA, Mader CW. Speed of sound in pure water. J Acoust Soc Am 1972;52:1442–1446.

Ebbini ES, Umemura SI, Ibbini M, Cain CA. A cylindrical-section ultrasound phase-array applicator for hyperthermia cancer therapy. IEEE Trans Ultrason Ferroelec Freq Control 1988;35:561–572.

Erikson KR, Fry FJ, Jones JP. Ultrasound in medicine—A review. IEEE Trans Sonics Ultrason 1974;SU-21:144–170.

Fry FJ. Transkull transmission of an intense focused ultrasonic beam. Ultrasound Med Biol 1977;3:179–184.

Fry FJ, Barger JE. Acoustical properties of the human skull. J Acoust Soc Am 1978;63:1576–1590.

Fry FJ, Goss SA. Further studies of the transkull transmission of an intense focused ultrasonic beam: Lesion production at 500 kHz. Ultrasound Med Biol 1980;6:33–38.

Fry WJ, Mosberg WH, Fry FJ. Production of focal destructive lesions in the central nervous system with ultrasound. J Neurosurg 1954; 11:471–478.

Guyott CCH, Cawley P. The measurement of through thickness plate vibration using a pulsed ultrasound transducer. J Acoust Soc Am 1988;83:623–631.

Hung B-N, Goldstein A. Acoustic parameters of commercial plastics. IEEE Trans Sonics Ultrason 1983;SU-30:249–254.

Hynynen K, Jolesz FA. Demonstration of potential noninvasive ultrasound brain therapy through an intact skull. Ultrasound Med Biol 1998;24:275–283.

Hynynen K, Sun J. Trans-skull ultrasound therapy: The feasibility of using image-derived skull thickness information to correct the phase distortion. IEEE Trans Ultrason Ferroelec Freq Control 1999; 46:752–755.

Kinra VK, Jaminet PT, Zhu C, Iyer VR. Simultaneous measurement of the acoustical properties of a thin-layered medium: The inverse problem. J Acoust Soc Am 1994;95:3059–3074.

Kinsler LE, Frey AR, Coppens AB, Sanders JV. Fundamentals of acoustics. 4th ed. New York: John Wiley & Sons, 2000.

Kremkau FW. Cancer therapy with ultrasound: A historical review. J Clin Ultrasound 1979;7:287–300.

Leisure RG, Willis FA. Resonant ultrasound spectroscopy. J Phys Condens Matter 1997;9:6001–6029.

Maynard J. Resonant ultrasound spectroscopy. Phys Today 1996;1:26–31.

Ohkawai H, Nitta S-I, Tanaka M, Dunn F. In vivo measurement of thickness or of speed of sound in biological tissue structures. IEEE Trans Sonics Ultrason 1983;SU-30:231–237.

Ophir J. Estimation of the speed of ultrasound propagation in biological tissues: A beam-tracking method. IEEE Trans Ultrason Ferroelec Freq Control 1986;33:359–368.

Pernot M, Aubry J-F, Tanter M, Thomas J-L, Fink M. Experimental validation of 3D finite differences simulations of ultrasonic wave propagation through the skull. In: Schneider SS, ed. Proceedings of the IEEE 2001 Ultrasonic Symposium. Piscataway: IEEE, 2001: 1547–1550.

Schwarz RB, Vuorinen JF. Resonant ultrasound spectroscopy: applications, current status and limitations. J Alloys Compd 2000;310: 243–250.

Seip R, VanBaren P, Ebbini ES. Dynamic focusing in ultrasound hyperthermia treatments using implantable hydrophone arrays. IEEE Trans Ultrason Ferroelec Freq Control 1994;41:706–713.

Strelitzki R, Clarke AJ, Evans JA. The measurement of the velocity of ultrasound in fixed trabecular bone using broadband pulses and single-frequency tone bursts. Phys Med Biol 1996;41:743–753.

Sun J, Hynynen K. Focusing of therapeutic ultrasound through a human skull: A numerical study. J Acoust Soc Am 1998;104:1705–1715.

Sun J, Hynynen K. The potential of transskull ultrasound therapy and surgery using the maximum available skull surface area. J Acoust Soc Am 1999;105:2519–2527.

Tanter M, Thomas J-L, Fink M. Focusing and steering through absorbing and aberrating layers: Application to ultrasonic propagation through the skull. J Acoust Soc Am 1998;103:2403–2410.

ter Haar G. Ultrasound focal beam surgery. Ultrasound Med Biol 1995;21:1089–1100.

Thomas J, Fink M. Ultrasonic beam focusing through tissue inhomogeneities with a time reversal mirror: Application to transskull therapy. IEEE Trans Ultrason Ferroelec Freq Control 1996;43: 1122–1129.

Vykhodtseva N, Sorrentino V, Jolesz FA, Bronson RT, Hynynen K. MRI detection of the thermal effects of focused ultrasound in the brain. Ultrasound Med Biol 2000;26:871–880.

Wells PNT. Biomedical ultrasonics. London: Academic Press, 1977.

Yapura CL, Kinra VK, Maslov K. Measurement of six acoustical properties of a three-layered medium using resonant frequencies. J Acoust Soc Am 2004;105:57–65.